Supplement of:

Remote sensing of aerosol water fraction, dry size distribution and soluble fraction using multi-angle, multi-spectral polarimetry

Bastiaan van Diedenhoven[1], Otto P. Hasekamp[1], Brian Cairns[2], Gregory L. Schuster[3], Snorre Stamnes[3], Michael Shook[3], and Luke Ziemba[3]

[1]SRON Netherlands Institute for Space Studies, Leiden, the Netherlands
[2]NASA Goddard Institute for Space Studies, New York, New York, USA
[3]NASA Langley Research Center, Hampton, Virginia, USA.

Correspondence: B. van Diedenhoven (b.van.diedenhoven@sron.nl)

1 Tables of daily statistics

For the 2020 winter and summer deployments of ACTIVATE and the 2019 CAMP^{2}Ex campaign, daily averages of water fraction, dry effective radius and variance and number concentrations (for particles with $D > 100$ μm) are shown in Table S1. Numbers in between brackets are standard deviations. Geometric averages and standard deviations are given for the number concentrations. In addition, the daily sulfate mass fraction derived from in situ observations and the soluble fraction retrieved by RSP are shown. Tables S2 and S3 gives the number of observations, observation time range and average latitude and longitude for the RSP and in situ data, respectively. In addition, table S2 shows daily averages and standard deviations of AOD, ambient effective radius and variance and refractive index retrieved by the RSP. Table S3 gives daily averages and standard deviations of the in situ-measured relative humidity, f(RH) and derived κ values.

Campaign	date	obs.	f_w	$r_{e,dry}$ [μm]	$v_{e,dry}$	N_a [cm^{-3}]	f_{sol} or $f_{m,sul}$
ACTIVATE winter 2020	28/02	I.S.:	0.23(0.28)	0.12(0.03)	-	228(2.23)	0.29
		RSP:	0.23(0.12)	0.17(0.02)	0.24(0.05)	128(1.43)	0.22
	29/02	I.S.:	0.14(0.18)	0.13(0.03)	-	264(4.77)	0.25
		RSP:	0.18(0.17)	0.15(0.02)	0.20(0.04)	299(1.26)	0.16
	01/03	I.S.:	0.15(0.23)	0.13(0.03)	-	251(3.43)	0.27
		RSP:	0.34(0.24)	0.17(0.02)	0.23(0.04)	170(1.38)	0.05
	09/03	I.S.:	0.29(0.29)	0.12(0.03)	-	178(2.66)	0.28
		RSP:	0.13(0.15)	0.14(0.02)	0.18(0.05)	176(1.37)	0.13
	11/03	I.S.:	0.27(0.22)	0.12(0.02)	-	429(2.38)	0.18
		RSP:	0.33(0.30)	0.15(0.01)	0.17(0.03)	125(1.48)	0.05
	12/03	I.S.:	0.39(0.25)	0.13(0.03)	-	199(4.17)	0.22
		RSP:	0.10(0.15)	0.15(0.02)	0.21(0.04)	263(1.65)	0.26
ACTIVATE summer 2020	17/08	I.S.:	0.41(0.25)	0.15(0.03)	-	101(2.98)	0.27
		RSP:	0.31(0.27)	0.16(0.03)	0.21(0.07)	296(1.66)	0.15
	20/08	I.S.:	0.33(0.14)	0.12(0.02)	-	686(1.86)	0.23
		RSP:	0.22(0.23)	0.16(0.02)	0.22(0.06)	375(1.59)	0.32
	21/08	I.S.:	0.42(0.13)	0.12(0.01)	-	367(4.07)	0.29
		RSP:	0.30(0.25)	0.17(0.02)	0.22(0.06)	292(1.57)	0.22
	02/09	I.S.:	0.19(0.09)	0.14(0.00)	-	595(1.21)	0.47
		RSP:	0.31(0.27)	0.15(0.02)	0.19(0.05)	268(1.59)	0.23
	23/09	I.S.:	0.07(0.10)	0.14(0.04)	-	406(2.45)	0.16
		RSP:	0.07(0.08)	0.17(0.01)	0.21(0.02)	283(1.30)	0.25
	29/09	I.S.:	0.21(0.23)	0.17(0.03)	-	119(3.08)	0.37
		RSP:	0.34(0.30)	0.15(0.03)	0.19(0.06)	186(1.45)	0.30
	30/09	I.S.:	0.32(0.25)	0.13(0.03)	-	184(3.99)	0.30
		RSP:	0.17(0.18)	0.17(0.02)	0.22(0.04)	171(1.35)	0.13
CAMP^{2}Ex 2019	27/08	I.S.:	0.54(0.20)	0.14(0.03)	-	166(4.50)	0.68
		RSP:	0.58(0.13)	0.14(0.02)	0.22(0.04)	258(1.41)	X
	30/08	I.S.:	0.26(0.20)	0.13(0.01)	-	376(2.10)	0.46
		RSP:	0.60(0.26)	0.15(0.01)	0.17(0.04)	357(1.39)	0.14
	04/09	I.S.:	0.19(0.22)	0.14(0.02)	-	486(3.33)	0.32
		RSP:	0.23(0.17)	0.17(0.01)	0.24(0.03)	267(1.21)	0.09
	06/09	I.S.:	0.20(0.18)	0.15(0.01)	-	747(3.50)	0.24
		RSP:	0.14(0.15)	0.16(0.01)	0.22(0.03)	573(1.24)	0.11
	08/09	I.S.:	0.15(0.15)	0.15(0.02)	-	233(3.36)	0.31
		RSP:	0.17(0.20)	0.15(0.02)	0.18(0.05)	242(1.28)	0.31
	13/09	I.S.:	0.50(0.30)	0.16(0.03)	-	264(4.57)	0.39
		RSP:	0.55(0.26)	0.13(0.02)	0.14(0.05)	176(1.77)	0.33
	15/09	I.S.:	0.00(0.01)	0.18(0.02)	-	1092(6.42)	0.12
		RSP:	0.02(0.03)	0.16(0.01)	0.26(0.03)	2406(1.53)	X
	16/09	I.S.:	0.15(0.25)	0.17(0.03)	-	442(6.03)	0.19
		RSP:	0.29(0.28)	0.14(0.01)	0.20(0.04)	533(1.33)	X
	19/09	I.S.:	0.44(0.21)	0.14(0.02)	-	346(2.41)	0.66
		RSP:	0.25(0.19)	0.21(0.03)	0.37(0.07)	310(1.18)	0.43
	21/09	I.S.:	0.33(0.17)	0.12(0.02)	-	568(2.16)	0.52
		RSP:	0.40(0.19)	0.14(0.02)	0.21(0.04)	468(2.00)	0.62
	23/09	I.S.:	0.44(0.14)	0.13(0.01)	-	676(1.83)	0.61
		RSP:	0.54(0.14)	0.12(0.01)	0.14(0.04)	495(1.30)	0.43
	27/09	I.S.:	0.61(0.23)	0.14(0.03)	-	73(1.63)	0.33
		RSP:	0.62(0.35)	0.12(0.04)	0.13(0.05)	132(1.29)	X
	01/10	I.S.:	0.32(0.17)	0.15(0.01)	-	961(1.60)	0.46
		RSP:	0.34(0.20)	0.13(0.02)	0.17(0.04)	644(1.77)	0.41
	03/10	I.S.:	0.32(0.14)	0.13(0.01)	-	833(3.19)	0.40
		RSP:	0.38(0.24)	0.13(0.01)	0.22(0.03)	1045(1.52)	X
	05/10	I.S.:	0.50(0.27)	0.15(0.04)	-	84(4.14)	0.65
		RSP:	0.51(0.24)	0.12(0.01)	0.17(0.02)	203(1.18)	X

Table S1. Daily averages and standard deviations (within brackets) of RSP and in situ data (see text for details)

Campaign	date	N_{obs}	time [h]	lat.	lon.	AOD	r_e [μm]	v_e	refr.
ACTIVATE winter 2020	28/02	33	15.4-20.9	34.3	-73.8	0.07(0.01)	0.19(0.02)	0.26(0.05)	1.49(0.02)
	29/02	110	14.8-17.5	37.8	-73.4	0.15(0.06)	0.16(0.02)	0.22(0.05)	1.51(0.05)
	01/03	69	14.1-19.3	37.1	-74.1	0.08(0.03)	0.19(0.03)	0.27(0.07)	1.47(0.05)
	09/03	277	17.2-19.1	33.7	-74.6	0.06(0.03)	0.15(0.03)	0.19(0.05)	1.52(0.04)
	11/03	62	13.5-15.0	36.4	-72.3	0.10(0.03)	0.17(0.02)	0.22(0.06)	1.49(0.08)
	12/03	35	17.1-20.0	35.9	-75.2	0.13(0.04)	0.15(0.02)	0.21(0.03)	1.54(0.05)
ACTIVATE summer 2020	17/08	173	15.0-17.6	37.6	-72.7	0.17(0.10)	0.19(0.05)	0.27(0.10)	1.48(0.06)
	20/08	430	14.6-17.1	37.4	-73.4	0.20(0.11)	0.18(0.04)	0.24(0.08)	1.50(0.06)
	21/08	441	14.3-16.8	37.3	-72.2	0.22(0.11)	0.20(0.04)	0.27(0.08)	1.48(0.06)
	02/09	103	16.4-16.8	33.6	-74.4	0.12(0.07)	0.17(0.04)	0.22(0.07)	1.50(0.05)
	23/09	545	18.5-20.0	37.1	-72.3	0.32(0.13)	0.17(0.01)	0.20(0.03)	1.53(0.04)
	29/09	42	15.3-16.4	37.7	-70.7	0.14(0.11)	0.19(0.07)	0.25(0.09)	1.48(0.08)
	30/09	340	16.4-19.3	38.0	-72.6	0.11(0.04)	0.19(0.03)	0.24(0.05)	1.51(0.05)
CAMP^{2}Ex 2019	27/08	30	4.0- 4.5	17.8	116.9	0.19(0.05)	0.19(0.03)	0.26(0.06)	1.42(0.04)
	30/08	35	26.9-27.8	8.3	119.6	0.19(0.05)	0.20(0.04)	0.27(0.08)	1.45(0.08)
	04/09	36	1.2- 1.6	9.3	117.7	0.14(0.03)	0.19(0.01)	0.29(0.05)	1.50(0.04)
	06/09	39	29.1-30.4	12.0	120.6	0.35(0.07)	0.17(0.02)	0.25(0.06)	1.52(0.04)
	08/09	15	26.7-26.8	18.5	123.3	0.12(0.04)	0.17(0.03)	0.23(0.05)	1.47(0.04)
	13/09	17	25.9-27.8	15.9	121.5	0.11(0.02)	0.18(0.02)	0.16(0.02)	1.49(0.03)
	15/09	43	27.0-28.8	9.1	119.4	0.84(0.15)	0.16(0.01)	0.25(0.04)	1.55(0.03)
	16/09	23	26.6-28.3	14.9	126.3	0.39(0.15)	0.17(0.02)	0.22(0.05)	1.53(0.06)
	19/09	24	29.7-29.9	18.2	122.6	0.32(0.05)	0.23(0.04)	0.37(0.08)	1.51(0.05)
	21/09	68	26.6-29.0	17.5	125.4	0.27(0.09)	0.17(0.02)	0.23(0.04)	1.48(0.06)
	23/09	100	24.7-26.8	17.8	126.1	0.19(0.05)	0.16(0.01)	0.21(0.02)	1.43(0.03)
	27/09	6	28.3-29.2	16.8	123.1	0.01(0.01)	0.21(0.02)	0.29(0.03)	1.47(0.01)
	01/10	65	26.4-27.9	19.7	120.6	0.18(0.10)	0.16(0.02)	0.20(0.05)	1.48(0.05)
	03/10	16	24.8-25.0	14.0	120.5	0.23(0.07)	0.16(0.01)	0.24(0.02)	1.46(0.05)
	05/10	5	2.1- 2.8	15.4	123.9	0.06(0.04)	0.17(0.03)	0.22(0.05)	1.44(0.05)

Table S2. Number of observations, observation time range and averages of latitude, longitude, effective radius, effective variance and refractive index retrieved by the RSP. Numbers in between brackets are standard deviations.

Campaign	date	N_{obs}	time [h]	lat.	lon.	RH [%]	f(RH)	κ
ACTIVATE winter 2020	28/02	3408	17.2-22.5	34.3	-73.3	72(17)	1.20(0.42)	0.12(0.18)
	29/02	7388	14.0-16.8	38.3	-72.4	70(13)	1.07(0.17)	0.05(0.05)
	01/03	3394	13.8-20.7	37.3	-73.1	66(16)	1.09(0.24)	0.06(0.09)
	09/03	4555	17.0-19.5	34.0	-74.8	70(19)	1.31(0.42)	0.15(0.19)
	11/03	7785	12.8-15.6	36.8	-73.4	81(9)	1.19(0.20)	0.09(0.09)
	12/03	10158	15.5-21.4	35.4	-73.6	81(9)	1.33(0.27)	0.15(0.12)
ACTIVATE summer 2020	17/08	5001	14.6-17.9	37.3	-72.8	84(7)	1.32(0.28)	0.15(0.13)
	20/08	1029	14.3-16.9	37.9	-73.1	67(12)	1.49(0.20)	0.23(0.10)
	21/08	1982	14.1-17.1	37.3	-73.1	70(7)	1.64(0.20)	0.30(0.10)
	02/09	264	15.8-15.9	35.7	-75.4	73(4)	1.20(0.12)	0.09(0.06)
	23/09	5776	18.0-20.2	37.1	-72.2	48(20)	1.09(0.16)	0.05(0.06)
	29/09	470	15.6-16.3	37.5	-70.9	69(16)	1.19(0.24)	0.10(0.10)
	30/09	5806	16.4-19.5	37.6	-73.5	76(13)	1.29(0.26)	0.14(0.12)
CAMP^{2}Ex 2019	27/08	5219	2.6- 5.7	17.7	117.6	85(6)	1.46(0.27)	0.21(0.13)
	30/08	5973	25.3-28.9	8.4	119.7	78(11)	1.19(0.17)	0.09(0.07)
	04/09	790	0.2- 2.6	8.3	119.4	77(12)	1.09(0.16)	0.05(0.07)
	06/09	2695	27.9-31.9	15.1	119.4	85(3)	1.11(0.12)	0.05(0.05)
	08/09	2824	27.1-28.2	18.6	123.6	79(8)	1.09(0.17)	0.05(0.07)
	13/09	2871	24.9-28.2	17.9	121.7	85(8)	1.43(0.27)	0.20(0.12)
	15/09	4625	25.4-28.1	8.5	118.6	77(8)	0.92(0.05)	0.00(0.01)
	16/09	3091	25.2-26.1	14.3	125.4	82(5)	1.10(0.24)	0.06(0.11)
	19/09	6463	28.2-31.4	17.8	122.2	80(7)	1.41(0.19)	0.19(0.09)
	21/09	4281	25.0-30.5	16.1	124.8	73(12)	1.35(0.17)	0.16(0.08)
	23/09	2662	27.6-28.4	17.8	127.3	82(6)	1.36(0.10)	0.17(0.05)
	27/09	1627	26.7-27.4	22.3	125.1	90(2)	1.49(0.34)	0.23(0.16)
	01/10	7292	24.9-29.5	20.1	120.8	77(9)	1.26(0.11)	0.12(0.05)
	03/10	5889	23.9-26.4	14.2	120.9	80(3)	1.27(0.16)	0.12(0.07)
	05/10	815	3.0- 4.1	15.8	125.2	86(4)	1.48(0.41)	0.23(0.19)

Table S3. Number of observations, observation time range and averages of latitude, longitude, relative humidity, f(RH) and κ obtained from in situ observations. Numbers in between brackets are standard deviations.

2 Refractive indices of binary aqueous mixtures of organics and ternary mixtures with organics and inorganic salts.

Here we analyze refractive indices of binary aqueous mixtures of organics and ternary mixtures with organics and inorganic salts as a function of volume water fraction. Refractive index and density data is obtained from Lienhard et al. (2012) (their Table 5). Figure S1 shows refractive indices for aqueous mixtures of levoglucosan and three aqueous mixtures of both levoglucosan and 1) ammonium sulfate, 2) ammonium nitrate and 3) ammonium bisulfate as a function of volume water fraction. In the ternary mixtures, the molar ratio of levoglucosan and salts were 1:1. The original data is given as a function of mass fraction of solute ($f_{m,s}$). Here we convert those fractions to volume water fractions (f_w) through

$$f_w = 1 - f_{m,s}\,\frac{\rho_{mix}}{\rho_{dry}}, \tag{1}$$

where ρ_{mix} is the density of the binary or ternary aqueous mixture given by Lienhard et al. (2012) and ρ_{dry} is the refractive index of the dry particles. For the mixtures with ammonium nitrate and ammonium bisulfate, ρ_{dry} is taken as the values at $f_{m,s} = 1$ provided by Lienhard et al. (2012). For the other mixtures, mass fractions close to unity were reported by Lienhard et al. (2012) and here we obtain densities at $f_{m,s} = 1$ by linear extrapolation. Also given in Fig. S1 (dashed lines) are the refractive indices obtained using the volume mixing rule. A linear least-squares fit through the data is used to obtained the dry refractive indices for those mixtures that did not extend all the way to $f_{m,s} = 1$ in the Lienhard et al. (2012) dataset. It can be seen that the volume mixing approach performs well in these cases of organic aerosol and ternary mixtures containing organic aerosol and inorganic salts. Similar results are obtained for other binary aqueous mixtures of organics reported by Lienhard et al. (2012). For reference, the refractive index of pure ammonium sulfate as provided by Tang and Munkelwitz (1991) is also given in Fig. S1 (red line). Here a dry density of 1.76 g/cm^3 is used (Erlick et al., 2011) to convert $f_{m,s}$ to f_w using Eq. 1. Note that this line is only plotted up to the critical mass fraction at which efflorescence occurs, assumed to be $f_{m,s} = 0.8$.

3 Effective refractive indices of external mixtures.

Remote sensing observations as presented in the main text, as well as in situ light scattering probes yield the effective refractive index of the observed population of aerosol particles, which may be externally mixed with several modes. A reasonable assumption may be that the effective refractive index is the optical depth-weighted average of those of the separate modes. In turn, as fine mode aerosol extinction roughly scales with its volume, the volume mixing mixing rule may yield a good approximation of the effective refractive index of external mixtures. To test this assumption, we calculate the single scattering properties of an external mixture of two aerosol modes with different refractive indices and then determine the refractive index of a single mode aerosol that is radiatively most equivalent to the external mixture, which can be considered as the effective refractive index of the mixture.

For this approach, Mie calculations are performed to calculate the phase matrices of non-absorbing aerosol modes with varying refractive indices. Subsequently, the phase matrices of two modes are added, weighted by the volume fractions and volume scattering efficiencies. The P_{12} element of the phase matrix is divided by the P_{11} element to obtain the degree of linear

polarization (DoLP). A radiatively equivalent single mode aerosol is then retrieved by finding the lowest root-mean-squared difference (RMSD) between the scattering properties (i.e. P_{11} and DoLP) of the external mixture and that of a single mode of which the refractive index is varied. Here, the RMSD is calculated for scattering angles between 90° and 165°.

To focus only on the real part of the refractive index, the size distribution is the same for both modes in the mixture and the single mode assumed for the effective refractive index retrieval, with a effective variance of 0.2 and effective radii of 0.12, 15, or 0.18 μm. One of the modes is assumed to have an refractive index of 1.54, while the refractive index of the second mode is varied between 1.33 and 1.54. These modes may be interpreted as respectively a insoluble mode and a soluble mode with a water fraction ranging from zero to unity assuming a volume mixing rule (cf. main text). The effective refractive index of the external mixture estimated using the volume fraction mixing rule is compared with the retrieved effective refractive index to assess the accuracy of using volume fraction mixing for the interpretation of the retrieved effective refractive index. Here, we focus on an equal fraction of the two modes (i.e., $f_{mode1} = 0.5$), since the maximum errors are expected for that case.

Figure S2 shows the differences between the estimated refractive index according to volume fraction mixing and that of the radiatively equivalent single mode aerosol. Volume mixing is shown to mostly underestimate the effective refractive index of the mixture. The absolute errors are shown to decrease as the difference between the refractive indices of the two modes decreases. Furthermore, the error depends on effective radius with largest errors for the small sizes. This behavior can be explained by the variation of the scattering efficiencies with size and refractive index, i.e. the error in the effective volume mixing refractive index increases as the difference in scattering efficiency of the two modes increases.

The errors in effective refractive index from assuming the volume mixing are relatively large at 0.035, 0.026 and 0.018 for the extreme case with an equal mixture of a purely dry aerosol mode and purely water aerosol mode, for effective radii of 0.12, 15, and 0.18 μm, respectively. In this case, the total volume water fraction estimated from the total refractive index under the assumption of the volume mixing rule would be 0.17, 0.13 and 0.09, respectively. However, we stress that these uncertainties must be considered as maximum values. For example, for an equal mixture of a purely dry aerosol mode and an aerosol mode containing 85% water (with refractive index of 1.365), errors in effective refractive index drop to 0.021, 0.013 and 0.006 for the three sizes, respectively, with representative errors in retrieved water volume fraction of less than 0.10, 0.06 and 0.03 for the three sizes, respectively. Furthermore, errors further decrease for mixing fractions deviating from 0.5. Hence, we can reasonably assume that the effective refractive index retrieved using multi-angle polarimetry is generally within about 0.02 of the volume-weighted refractive index of the externally mixed aerosol. Moreover, for our purpose of inferring volume water fraction from the retrieved effective refractive indices, the mixing state of the aerosol is generally irrelevant.

References

Erlick, C., Abbatt, J. P. D., and Rudich, Y.: How Different Calculations of the Refractive Index Affect Estimates of the Radiative Forcing Efficiency of Ammonium Sulfate Aerosols, Journal of Atmospheric Sciences, 68, 1845–1852, https://doi.org/10.1175/2011JAS3721.1, 2011.

Lienhard, D. M., Bones, D. L., Zuend, A., Krieger, U. K., Reid, J. P., and Peter, T.: Measurements of Thermodynamic and Optical Properties of Selected Aqueous Organic and Organic–Inorganic Mixtures of Atmospheric Relevance, The Journal of Physical Chemistry A, 116, 9954–9968, https://doi.org/10.1021/jp3055872, pMID: 22974307, 2012.

Tang, I. N. and Munkelwitz, H. R.: Simultaneous Determination of Refractive Index and Density of an Evaporating Aqueous Solution Droplet, Aerosol Science and Technology, 15, 201–207, https://doi.org/10.1080/02786829108959527, 1991.

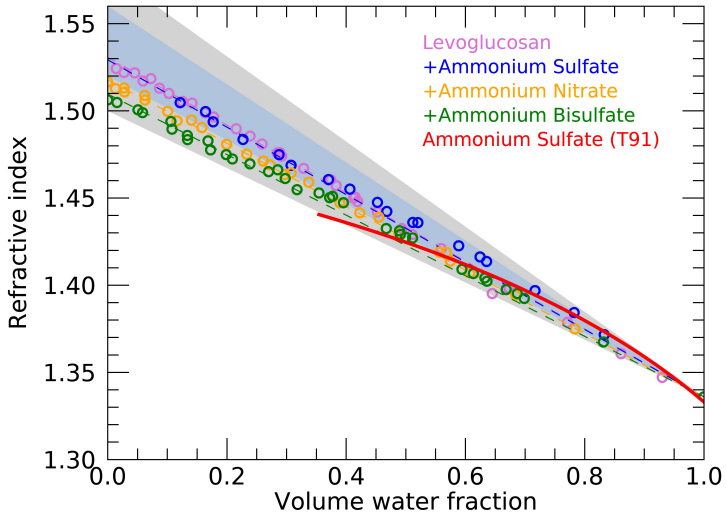

Figure S1. Refractive mixture of binary solutions of levoglucosan and water and three ternary solutions of levoglucosan, water and inorganic salts, as indicated by the different colors. Dots are derived from observations of Lienhard et al. (2012), while dashed lines are approximations using the volume mixing rule. The red line represents the parameterized refractive index of pure ammonium sulfate provided by Tang and Munkelwitz (1991). Blue and grey areas are ranges obtained by applying the volume mixing rule to $n_{dry} = 1.54 \pm 0.02$ and $n_{dry} = 1.54 \pm 0.04$, respectively.

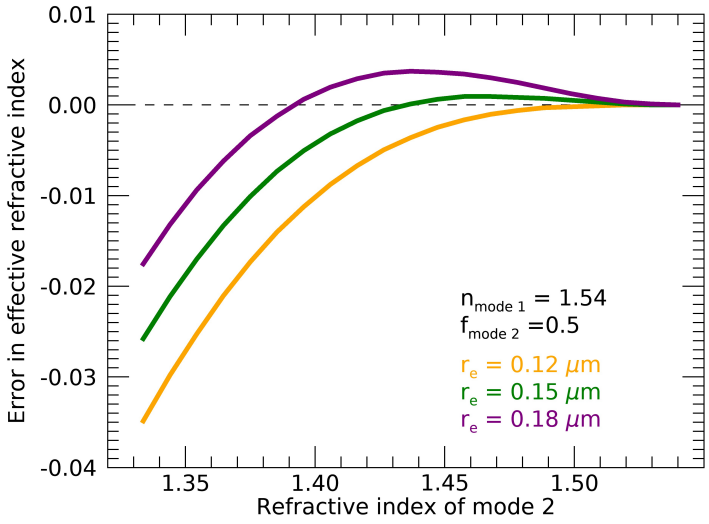

Figure S2. Error in effective refractive index of a two-mode aerosol mixture from applying the volume fraction mixing rule as a function of the refractive index of one of the modes. The other mode is assumed to have a refractive index of 1.54. An equal fraction of the two modes is assumed. Results are shown for aerosols with size distributions with a effective radius of 0.12 (orange), 0.15 (green) and 0.18 (purple) μm.